Initial Stages of Influenza Hemagglutinin-induced Cell Fusion Monitored Simultaneously by two Fluorescent Events: Cytoplasmic Continuity and Lipid Mixing

Debi P. Sarkar,* Stephen J. Morris,*‡ Ofer Eidelman,*§ Joshua Zimmerberg,‖ and Robert Blumenthal*

*Section on Membrane Structure and Function, LTB, National Cancer Institute, National Institutes of Health, Bethesda, Maryland 20892; ‡Division of Molecular Biology and Biochemistry, School of Basic Life Sciences, University of Missouri at Kansas City, Kansas City, Missouri 64110; §Department of Biological Chemistry, Hebrew University, Jerusalem, Israel; and ‖Section on Biological Physics, LBM, National Institute of Diabetes and Disorders of the Kidney, and Physical Sciences Laboratory, Division of Computer Research and Technology, National Institutes of Health, Bethesda, Maryland 20892

Abstract. We have monitored the mixing of both aqueous intracellular and membrane-bound fluorescent dyes during the fusion of human red blood cells to influenza hemagglutinin-expressing fibroblasts using fluorescence spectroscopy and low light, image-enhanced video microscopy. The water-soluble fluorescent dye, *N*-(7-nitrobenzofurazan-4-yl)taurine, was incorporated into intact human red blood cells. The fluoresence of the dye in the intact red blood cell was partially quenched by hemoglobin. The lipid fluorophore, octadecylrhodamine, was incorporated into the membrane of the same red blood cell at self-quenching concentrations (Morris, S. J., D. P. Sarkar, J. M. White, and R. Blumenthal. 1989. *J. Biol. Chem.* 264: 3972–3978). Fusion, which allowed movement of the water-soluble dye from the cytoplasm of the red blood cell into the hemagglutinin-expressing fibroblasts, and movement of octadecylrhodamine from membranes of red blood cell to the plasma membrane of the fibroblasts, was observed by fluorescence microscopy as a spatial relocation of dyes, and monitored by spectrofluorometry as an increase in fluorescence. Upon lowering the pH below 5.4, fluorescence increased after a delay of about 30 s at 37°C, reaching a maximum within 3 min. The kinetics, pH profile, and temperature dependence were similar for both fluorescent events measured simultaneously, indicating that influenza hemagglutinin-induced fusion rapidly establishes bilayer continuity and exchange of cytoplasmic contents.

It is now well-documented that spike glycoproteins on the viral membrane surface are responsible for the ability of enveloped viruses to invade host cells (Choppin and Scheid, 1980; White et al., 1983). Influenza virus, which normally first binds to sialic acids on the cell surface and then enters via the endocytic pathway, can be made to fuse to the plasma membrane by briefly lowering the pH of the medium after the virus is attached to the cell (White et al., 1981). The influenza virus hemagglutinin (HA)[1] is the best characterized integral membrane glycoprotein that mediates membrane fusion (Wiley and Skehel, 1987).

To study initial steps of viral fusion, we chose to analyze a cell culture model for HA-induced membrane fusion. Lines of bovine papilloma virus-transformed NIH3T3 cells have been developed that constitutively express HA in large quantities (>5 × 10^5 copies/cell) on the cells' surface (Sambrook et al., 1985). Expression of membrane fusion activity in this cell line has been shown by delivery of the contents of red cell ghosts into the cells' cytoplasm (Doxsey et al., 1985). A subclone of a line of HA-expressing fibroblasts (GP4F cells) has been selected that expresses HA at high surface density and adheres tightly to its growth substrate (Ellens, H., D. Mason, and J. M. White, manuscript in preparation). This system offers the advantages of producing large amounts of material for spectroscopic assays, microscopic imaging, and electrophysiological measurements.

Using an assay based on the relief of self-quenching of fluorescence of the membrane marker, octadecylrhodamine (R18) (Hoekstra et al., 1984), we have recently measured the kinetics and extent of fusion between the GP4F cells and human red blood cells (RBC) (Morris et al., 1989). A number of control experiments demonstrated the specificity of the R18 assay. However, since R18 would be expected to primarily insert into the outer leaflet of the RBC bilayer lipids, it is possible that the influenza HA induced only "partial" fusion of the outer leaflets. Therefore, we developed a second method, based on cytoplasmic mixing, which would continuously report a different criterion of fusion. By using RBC

1. *Abbreviations used in this paper*: FDQ, fluorescence dequenching; HA, influenza hemagglutinin; NBD-taurine, *N*-(7-nitrobenzofurazan-4-yl)taurine; R18, octadecylrhodamine; RBC, human red blood cell.

simultaneously labeled with both a cytoplasmic and a membrane marker, we could directly measure the kinetics, pH-profile, and temperature-dependence of fusion by measuring both events simultaneously by spectrofluorometry. Moreover, by using low light level video microscopy and image enhancement techniques, we followed the spatial relocation of both dyes in single cells during the fusion process.

Materials and Methods

Materials

Octadecyl rhodamine B chloride (R18) and *N*-(7-nitrobenzofurazan-4-yl)taurine (NBD-taurine) was obtained from Molecular Probes (Junction City, OR); Triton X-100 from Aldrich Chemical Co. (Milwaukee, WI); Cell culture media and Trypsin-EDTA were obtained from Gibco Laboratories (Grand Island, NY). Neuraminidase (type V) and Trypsin (type XII-S) were obtained from Sigma Chemical Co. (St. Louis, MO).

Cell Cultures

A subclone (HA-expressing fibroblasts [GP4F]) of a line of bovine papilloma virus-transformed NIH3T3 cells that constitutively expresses HA from the influenza virus strain A/Japan/305/57 (H2N2) was grown as described previously (Morris et al., 1989).

Incorporation of Fluorescent Probes into RBC

Labeling of RBC with R18 was carried out as described previously (Morris et al., 1989). Entrapment of NBD-taurine followed the method of Eidelman and Cabantchik (1980): fresh human RBCs were collected from volunteer donors through the National Institutes of Health blood bank. RBCs were washed three times with 137 mM NaCl, 2.7 mM KCl, 8.1 mM Na_2HPO_4, 1.5 mM KH_2PO_4, pH 7.4 (PBS) and finally suspended in PBS at 1% hematocrit. 10 ml was pelleted at 300 *g* for 10 min at 4°C. The pellet was suspended in 1 ml of 10 mM NBD-taurine in PBS and incubated at 37°C for 30 min to allow NBD-taurine uptake, presumably via the RBC anion transporter (Eidelman et al., 1981). The cell suspension was cooled in ice for 5 min. To block efflux of NBD-taurine after entrapment, RBCs were treated with 4,4′-diisothiocyantodihydrostilbene 2,2′-disulfonic acid, which is known to irreversibly inhibit anion transport (Cabantchik and Rothstein, 1972). The cells were washed twice with a 100 mM Na_2SO_4 and 10 mM Hepes buffer, resuspended in the same buffer containing 0.5 mM 4,4′-diisothiocyantodihydrostilbene 2,2′-disulfonic acid; the suspension was left at 4°C for 10 min, and then incubated at 37°C for 20 min. At the end of the incubation, cold DME containing 10% heat-inactivated FBS was added to a final volume of 50 ml, and the RBC washed with 50 ml cold PBS. The cells were finally suspended in 10 ml cold PBS and could be stored for up to a week at 4°C without much loss of fluorophore. The fluorescence of the NBD-taurine inside the RBC is known to be quenched by hemoglobin (Eidelman and Cabantchik, 1980); release of the probe into the medium upon addition of 0.1% Triton X-100 resulted in a three- to sixfold increase in fluorescence. Leakage of NBD-taurine into the medium during RBC–GP4F fusion was assessed using anti-NBD antibodies, which quench NBD fluorescence upon binding (Darmon et al., 1982). When NBD-taurine–loaded RBC were permeabilized by low concentrations of detergent all the NBD-fluorescence disappeared as observed by fluorescence microscopy. This indicates that the molecule does not bind to membranes under the experimental conditions employed.

RBC were labeled with both R18 and NBD-taurine using the same procedure as for entrapment of NBD-taurine, except that 15 μl of 1 mg/ml R18 in ethanol was added to the incubation of 10 mM NBD-taurine at 37°C. After labeling, the RBC suspension was incubated with DME containing 10% heat-inactivated FBS for 20 min at room temperature. The suspension was washed six times with 50 ml PBS (each time in a clean tube) to remove unincorporated R18 and NBD-taurine. The double-labeled RBC were stored at 4°C for up to a week. They showed the same amounts of fluorescence quenching and stability for each dye as their single-labeled counterparts.

Binding of RBC to GP4F Cells

The binding of RBC to GP4F cells was performed as described previously (Morris et al., 1989). Fibroblasts (~2 × 10^7 cells) growing in 250-ml (Costar, Cambridge, MA) flasks were treated with 5 ml of 5 μg/ml trypsin and 0.22 mg/ml neuraminidase in PBS for 10 min at room temperature. The HA is initially synthesized as a single polypeptide precursor HAo that is fusion inactive (Klenk et al., 1975). The 5 μg/ml trypsin is sufficient to cleave HAo and render the GP4F cells fusogenic (Morris et al., 1989). The attached cells were rinsed, and a 5-ml suspension of labeled RBC (0.1% hemocrit) in PBS was added. The flask was incubated at room temperature for 10 min with occasional gentle agitation to form RBC–GP4F complexes. Unbound RBC were removed by gently running PBS solution over the cells during three rinses and aspirating. Attached decorated cells were then lifted from the flask with a solution of 0.5 mg/ml trypsin and 0.2 mg/ml EDTA, washed, and placed on ice until use. About 3 RBC/GP4F cell remained bound; this ratio could be adjusted by varying the number of the RBC added to the activated GP4F cells, and varying the incubation time. In control experiments, cells were treated with only neuraminidase before RBC binding and removed from the flasks with chymotrypsin (0.5 mg/ml) containing 0.2 mg/ml EDTA in PBS, to avoid cleaving HAo.

Light Microscopy

3 μl of cells suspended in PBS containing 2 mM Ca^{2+}, 2 mM Mg^{2+}, and 1 mM *n*-propyl gallate were placed within a 10 mm raised circle printed onto a microscope slide (Roboz Surgical Instrument Co. Inc., Washington, D.C.) covered with an 18 × 18 mm No. 1 cover slip and examined using a 100 ×/1.3 oil immersion objective (Plan-Neofluor, Carl Zeiss, Inc., Thornwood, NY) on a microscope, (Axioplan; Carl Zeiss, Inc.) either by phase contrast, differential interference contrast, or epifluorescence. Cells were photographed (Ektachrome 160 or Tri-X-pan film; Eastman-Kodak Co., Rochester, NY). NBD fluorescence was visualized using a "fluorescein" filter set (450-490 excitation filter, ft 510 dichroic mirror, and lp 520 emission filter, Carl Zeiss, Inc.). R18 fluorescence was observed with a "rhodamine" filter set (BP 546 excitation filter, ft 580 dichroic mirror, and lp 590 emission filter). No spectral overlap was observed except for an occasional reddish outline on the double-labeled cells when viewing the NBD-fluorescence.

Cells strongly irradiated with fluorescent light bleached rapidly, and began to bleb after some minutes. Addition of 1 mM *n*-propyl gallate in the suspension medium greatly reduced photobleaching (Giloh and Sedat, 1982), but did not stop blebbing. The *n*-propyl gallate at that concentration did not affect the kinetics of fusion measured by spectrofluorometry. To minimize photodynamic damage, incident excitation light was adjusted to the lowest possible level with neutral density filters. No blebbing was seen at this incident light level.

The micrographs in Fig. 1 have been chosen to show one RBC bound to a single fibroblast about the equator of the spherical cell in suspension. However, if two or more RBC are bound, it becomes important to examine the complexes at several levels of focus to reveal all bound RBCs.

Video Microscopy

Video microscopy was performed using a modified inverted microscope (model IM405; Carl Zeiss, Inc.). A polylysine-coated, No. 0 coverslip fragment was placed on the No. 0 glass coverslip bottom of a 25-mm-diam, teflon, temperature-controlled chamber containing 1.0 ml of PBS. Temperature was controlled at 37 ± 0.4°C with a 100 μm thermistor placed in the solution near the cell under observation. 20 μl of a concentrated suspension of decorated cells were added from a pipette (Eppendorf pipettes made by Brinkmann Instruments, Inc., Westbury, NY), and the cells were allowed to settle on to the coverslip. The microscope was focused using illumination (Koehler Instrument Co., Inc., Bohemia, NY) with reduced light intensity for bright field. The image was formed on a ksl380 multichannel intensifier plate (Videoscope International Ltd., Washington, DC) and was displayed and recorded on a video monitor and a three-quarter inch video recorder (Trident Electronics Co., Fremont, CA). The incandescent lamp was turned off and the specimen was refocused to view the R18 or NBD fluorescence, using the same filter sets noted above. The real time clock was started. The pH was lowered by adding over a 5–10 s period 1.0 ml of a PBS-citrate buffer at pH 5 and 37°C.

The videotape was analyzed by means of an imaging computer (model FG151; Image Technology, Woburn, MA). Thirty two frames (1.06 s) of data were averaged as described in the legend to Fig. 3, to give maximum contrast. The same section of each averaged frame was arranged in a montage (see Fig. 3, *A* and *B*).

Spectrofluorometric Measurements

Spectrofluorometric measurements were made using a spectrofluorometer (model 8000; SLM Instruments Inc., Urbana, IL) with 1-s time resolution.

Excitation and emission wavelengths were 473 and 515 nm for NBD and 560 and 590 for rhodamine. High pass filters (models OG 515 and OG 570; Schott America Glass & Scientific Products, Inc., Yonkers, NY) were placed in the emission optical path for NBD and rhodamine to reduce scatter. The standard kinetic fusion assay was performed as follows: 2 ml of PBS were prewarmed to 37°C, placed in a disposable plastic fluorescence cuvette, and stirred with a 2 × 8-mm teflon-coated flea. 20–50 μl of the R18RBC-GP4F suspension was added and allowed to equilibrate to the temperature. The pH in the cuvette was changed by rapidly injecting 5–50 μl of 0.5 M citric acid. The mixing time was 3–4 s as measured by the reduction in fluorescence quantum yield of 2 ml of a solution of carboxyfluorescein in PBS upon adding 20 μl of 0.5 M citrate. The pH of the solution in the cuvette was always measured at the end of the experiment using a pH meter (model 811; Orion Research Inc., Cambridge, MA).

Percent fluorescence dequenching (FDQ) at any time period was calculated according to:

$$\%\text{FDQ} = \frac{F - F_0}{F_t - F_0} \times 100, \quad (1)$$

where F_0 and F are the fluorescence intensities at time 0 and at a given time point (Blumenthal et al., 1987). F_t is the fluorescence after disruption of cells by the detergent Triton X-100, which results in essentially infinite dilution of the probe.

For NBD-taurine, the calculations were complicated by leakage (see below). Therefore, duplicate assays were performed in the presence or absence of anti-NBD antibody (Darmon et al., 1982). Sufficient antibody was added to completely quench NBD fluorescence after lysing the cells with Triton X-100. The analysis of the leakage correction is described in Appendix I.

Results

Light Microscopy

RBC labeled with NBD-taurine and octadecylrhodamine were bound to GP4F cells as described in Materials and Methods. They were photographed with the fluorescein filter set (Fig. 1, *b* and *f*), the rhodamine filter set (Fig. 1, *c* and *g*), and double-exposed with both (Fig. 1, *d* and *h*).

The examples in Fig. 1 were chosen to show single RBCs attached to single GP4F cells. However, the number of attached RBC varied with each preparation and could be additionally varied from <1:1 to >10:1 by manipulating the starting ratios of the two cell types and the binding time. At pH 7.4, the fluorescence of NBD-taurine was diffusely distributed within the cytoplasm of the RBC, and that of R18 was diffusely distributed over the RBC surface (Fig. 1, *b–d*). RBC-GP4F complexes incubated at pH 7.4 37°C, for 30 min showed no redistribution of either fluorescent label. Even cells incubated at 4°C for 72 h showed no redistributions of dyes.

Membrane fusion of cells bearing this strain of influenza virus is triggered at pH < 5.3 (White et al., 1982). When the RBC–GP4F complexes were subjected to pH 5 for 30 s, returned to a pH 7.4 buffer and examined after 2 min, the NBD-taurine was seen redistributed into the cytoplasm (Fig. 1, *f* and *h*) of the GP4F cells and the R18 over its surface (Fig. 1, *g* and *h*). In samples exposed to low pH for more than 2 min, probe redistribution had occurred in virtually every complex. However, cells incubated for longer times did not seem to retain the NBD-taurine. Instead, the background around a cell would brighten gradually while the fluorescence in the GP4F cell dimmed; in some cases, the fibroblast would suddenly go dark at longer times. These results are discussed below in relation to the leakage of NBD observed fluorimetrically. Fig. 1 *h* shows that double-labeled RBC attached to GP4F cells led to redistribution of both probes after incubation at pH 5 and 37°C, indicating that influenza hemagglutinin activation induces both membrane mixing and cytoplasmic continuity, as expected for a fusion event.

Although NBD-taurine redistribution occurred within 3 min after pH-activation, the RBC retained their hemoglobin for >10 min as judged by the retention of pink absorbing material (Fig. 2). We also observed RBC swelling after pH activation; this was not seen in cells kept at pH 7 for this period or for HAo controls at pH 5.

Low Light Level Video Microscopy

To observe probe redistribution at low light level after pH activation of single cells, we modified the video microscopy system that had been used to follow continuously the exocytosis of mast cell granules (Zimmerberg et al., 1987). Fig. 3 shows the time-dependent redistributions of both dyes into the GP4F cells when RBC labeled with NBD-taurine and R18 fuse after lowering the pH from 7 to 5.

Two cells are shown in the case of R18 redistribution (Fig. 3 *A*). Movement of the dye was seen in ~50 s after lowering the pH as indicated by a brightened fluorescence in the interfacial region between RBC and GP4F membranes; complete redistribution was seen ~60 s later. This movement is consistent with a lipid diffusion coefficient of $\sim 10^{-8}$ cm²/s (see Discussion).

In contrast, the NBD-taurine appeared to be redistributed homogeneously throughout the GP4F cell immediately after crossing the RBC–GP4F barrier, although its total fluorescence in the GP4F cell increased slowly (Fig. 3 *B*). The instantaneous NBD-taurine redistribution in the GP4F cell is consistent with a diffusion coefficient of $\sim 5 \times 10^{-6}$ cm²/s of the small aqueous fluorophore (see Discussion). On the other hand, the slow increase in total NBD fluorescence relative to that expected for free diffusion of this fluorophore, in the GP4F cells is because of limited permeability across the "junction" formed by fusion complexes. This limited permeability provided a constraint for hypothetical structures of this junction (see Discussion).

Kinetics of Fusion and Leakage Monitored Fluorimetrically

To obtain information about the rates and extents of HA-induced fusion, we measured the kinetics of dequenching of NBD-taurine fluorescence from intact RBC. Fig. 4 shows that at pH 5.0, fluorescence increased sigmoidally after ~30-s delay reaching a value in 3 min that corresponds to ~100% fluorescence dequenching (see below).

As had been observed by fluorescence microscopy (Figs. 1–3), fusion allowed movement of NBD-taurine from RBC into GP4F cells. The increased fluorescence signal is because of the escape of NBD-taurine from the hemoglobin environment. However, the fluorescence increase could be the result of escape of dye into the medium resulting from leakage in addition to fusion.

To resolve these two contributions to the signal, we added an antibody to NBD to the medium that quenches its fluorescence. Fig. 4 shows that the signal was decreased by ~30% in the presence of antibody. This result indicates that ~30% of the fluorescence change is because of leakage. The spectrofluorimetric assay does not resolve whether there was 30% NBD-taurine leakage from each RBC, or 30% of the RBCs showing complete leakage upon initiation of fusion.

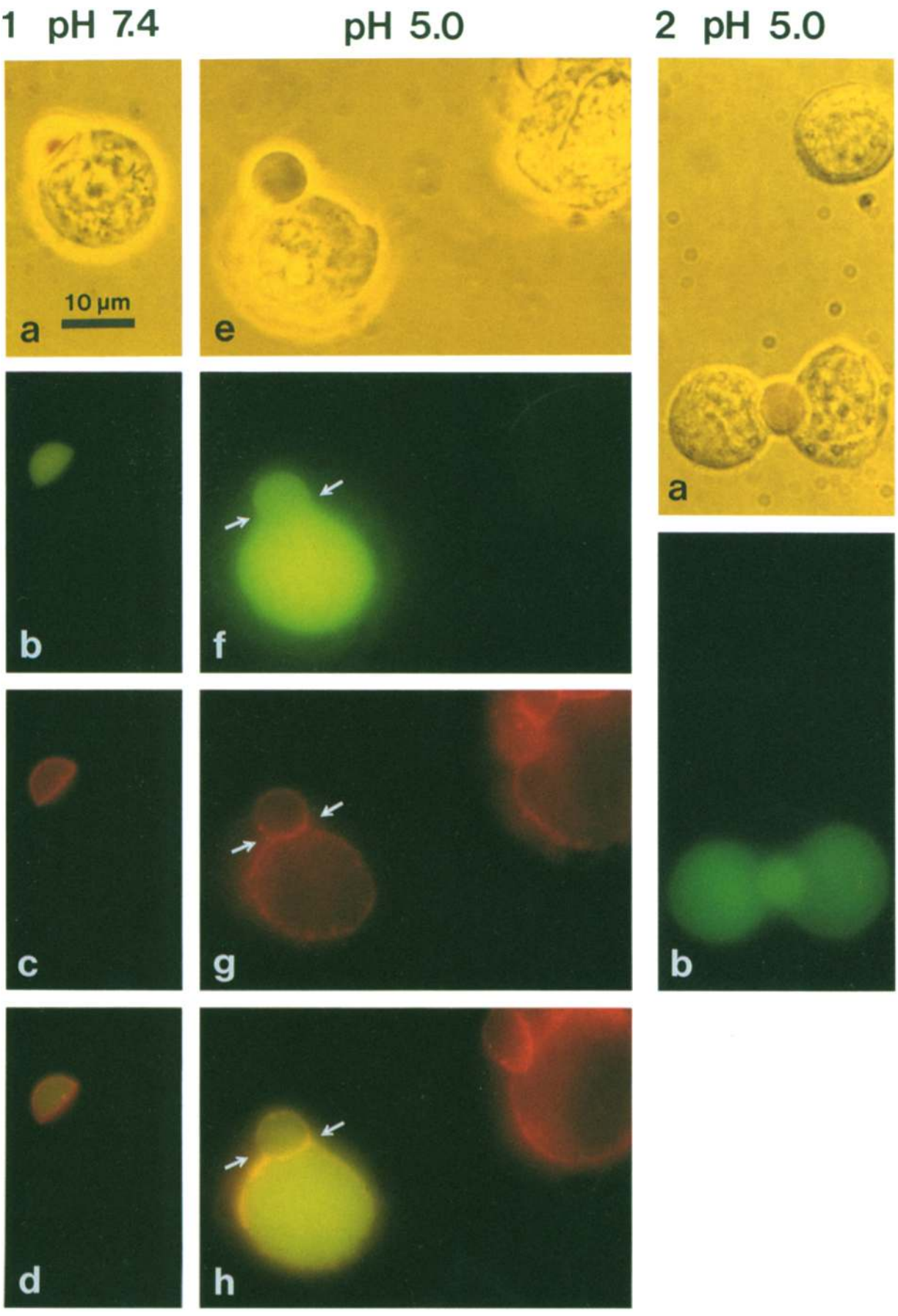
1 pH 7.4
pH 5.0
2 pH 5.0
10 μm
a
e
a
b
f
b
c
g
c
d
h
d

However, by video microscopy we do not see disappearance of NBD fluorescence from the fusing RBCs either at the onset or after R18 redistribution, as predicted by the latter hypothesis. It therefore appears that leakage from each RBC occurs at the onset of fusion.

We had previously shown that no fusion occurs with cells expressing the uncleaved precursor hemagglutinin (HAo) as measured by R18-dequenching (Morris et al., 1989). To establish that the mere binding of RBC to GP4F is insufficient for the transfer or leakage of the aqueous dye at pH 5, NBD-taurine–loaded RBCs were bound to HAo-expressing GP4F cells. No fluorescence increase was observed despite incubation at 37°C and low pH (Fig. 4), indicating that the dye leakage followed the same pattern as HA-induced fusion. The similar kinetics of HA-induced leakage and fusion indicate that the leakage is caused by a permeability change in the RBC membrane during fusion (see Discussion) and not by the NBD-taurine escaping through the GP4F membrane after entry into the GP4F cell.

Comparison between Cytoplasmic-mixing and Lipid-mixing

After subtracting the leakage component, the specific contribution of the NBD-taurine to cytoplasmic-mixing can be calculated according to the equations developed in Appendix I. Fig. 5 shows that when the leakage correction has been made, the FDQ of NBD-taurine reached ~80%. Fig. 5 shows a comparison between FDQ of NBD-taurine and R18, with doubly labeled cells. The FDQ seen with R18 was only ~20%. We have previously discussed possible low values for FDQ with the R18 (Morris et al., 1989). Since the ratio in surface areas between the two cells is ~6:1, fusion of more than one RBC/GP4F cell will result in insufficient dilution of R18 for maximal dequenching. This experiment demonstrates that the amount of fusion is underestimated using R18. By normalizing the R18 curve to the maximal extent of FDQ of NBD-taurine, it appears that the rate of R18-dequenching was slightly faster. However, the lag time and the sigmoidicity of the fluorescence change were about the same when two entirely different dyes probing different criteria of fusion were used.

Since both fusion and leakage are HA-dependent phenomena, and since the leakage had similar kinetics as the fusion, we present the following data on NBD-taurine dequenching, which are uncorrected for leakage.

Temperature Dependence

Temperature-dependence of NBD-taurine fluorescence dequenching at pH 5.0 is shown in Fig. 6. Both the delay in onset and the maximal rate of dequenching were affected by temperature. However, the maximal extents of NBD-taurine FDQ dequenching were the same at the different temperatures. For comparison, the temperature dependence of R18-dequenching using doubly labeled RBCs is shown (Fig. 6). Again, the maximal extents of fluorescence dequenching of R18 were considerably less than those of NBD-taurine. However, at each temperature measured, the lag in the onset of fusion measured with NBD-taurine was the same as that measured with R18. This experiment clearly demonstrates that the lag in onset previously observed (Morris et al., 1989) is not because of dye diffusion as a rate-limiting step; rather, the lag appears to be the result of initial events following pH activation of HA preceding lipid continuity and cytoplasmic mixing.

pH Dependence

Fig. 7 *A* shows the pH dependence of NBD-taurine dequenching. The time lag and the rates were pH dependent with a threshold of about pH 5.4, with about the same extents. Fig. 7 *B* shows the maximal rates of FDQ as a function of pH both for NBD-taurine and for R18, using doubly labeled cells. The pH dependence of these rates was very similar to that of syncytium formation induced by the same strain of influenza virus (White et al., 1982).

Discussion

Measurement of Membrane Fusion by Two Fluorescence Events

In defining membrane fusion, it is necessary to establish the continuity of the aqueous compartments defined by the membranes and the lipid compartments comprising the membranes of two previously separated structures (Zimmerberg

Figure 1. Fusion of GP4F with human RBC as detected by fluorescence microscopy. *a* shows a double-labeled RBC attached to a GP4F cell in phase contrast incubated at pH 7.4 for 90 s, and then whole mounted and examined as described in the Materials and Methods section. *b–d* are NBD, R18, and double-exposure fluorescence photos of the same cell. Note that the fluorophores are confined to the RBC cytoplasm and membrane respectively; there is no transfer of either label to the fibroblast, except under conditions that trigger fusion. *e–h* are photos of two double-labeled RBC-decorated cells after 90 s, pH 5.0 at 37°C. Note the swelling of the RBC (typical photodynamic damage [see text]) and the redistribution of NBD in the cell (*left*). The cell (*right*) is brightly labeled with R18 (*g–h*) but lacks NBD, suggesting that it has lysed (see text). The opposing arrows show that the double membrane, seen in *g* and *h* is lacking in *f*, in keeping with the cytoplasmic distribution of NBD. The rhodamine fluorescence appears yellow in *h*, because of the overlying green of the NBD.

Figure 2. Hemoglobin does not move from RBC to GP4F after fusion detected by NBD-taurine movement. The photos were chosen from a series in which NBD-taurine labeled RBC were attached to GP4F and the pH was reduced as in Fig. 1, *e–h*. A single GP4F cell to which no RBCs are attached is seen in *a* (*top*), and a single RBC attached to two GP4F cells is seen in *a* (*bottom*). *b* shows NBD fluorescence; both photographs were taken after fusion had been triggered at pH 5.0. Note that although the RBC is swollen, it has not lost its hemoglobin, which appears pink (*a*). Similar results were seen in R18 and double-labeled cells. An NBD experiment was chosen since in some cases the R18 concentrations in the RBC were high enough to make the cells appear reddish, even after lysis. NBD-labeled RBC appear colorless after lysis. Also note the absence of NBD in the upper cell, to which no RBC is attached. There is no nonspecific uptake or transfer of NBD to such cells.

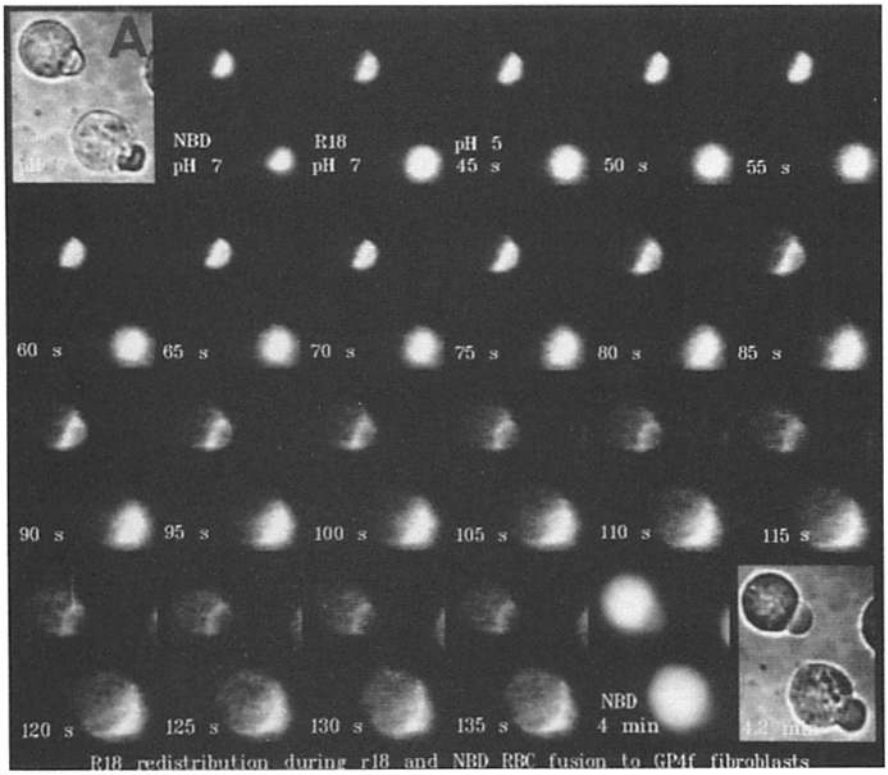

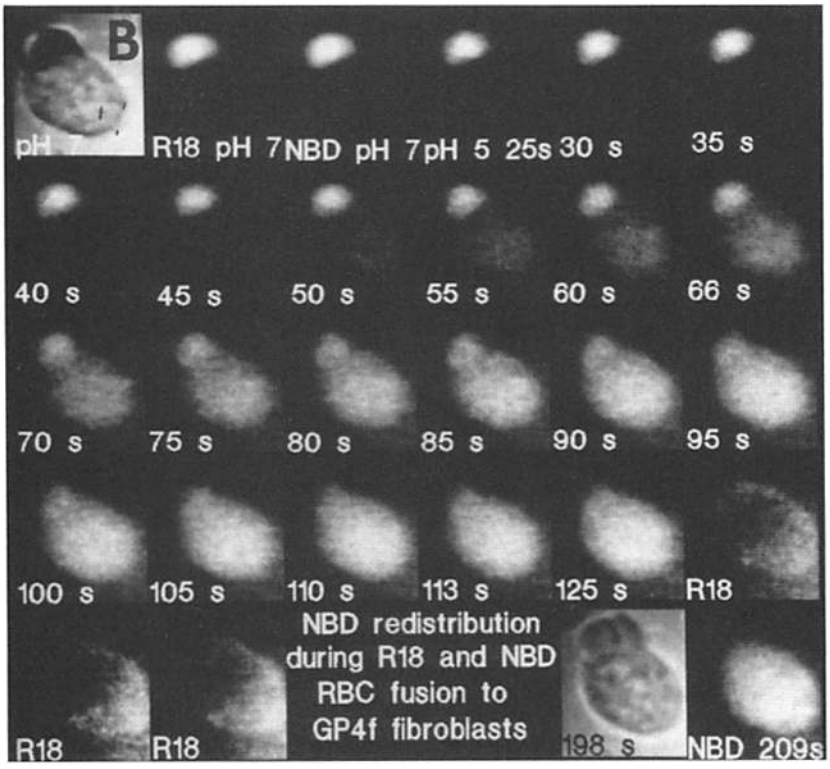

Figure 3. Processed images of RBC-GP4F fusion as detected by low light level fluorescence video microscopy. GP4F were treated with trypsin/neuraminidase, decorated with double-labeled RBC, and bound to polylysine-coated coverslips in 1.0 ml of PBS, pH 7.4, in the environmental chamber of the inverted microscope as described in Materials and Methods. When the temperature reached 37°C, the pH was changed to 5.0 over 5–10 s by the addition of PBS containing citric acid. Fusion events began 30–45 s later as would be expected from the lag period at this temperature. Within the lag period, bright field, NBD, and rhodamine fluorescence was recorded and one of the two fluorophores was followed for the next 5–10 min. The time in seconds after the pH change is noted at the bottom of the frames. (*A*) Bright field, NBD, and rhodamine fluorescence redistribution. (*B*) A similar experiment in which NBD redistribution is followed. An average of eight frames (267 millis) was used for the bright field images and 32 frames (1.06 s) for the fluorescent images. This entire plate was contrast enhanced with the same grey scale.

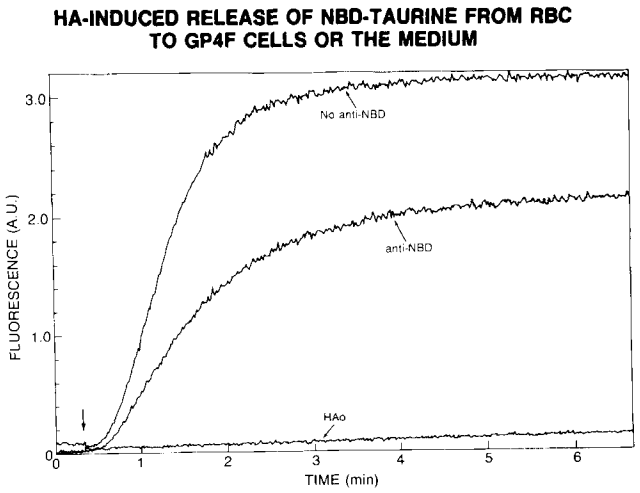

Figure 4. Kinetics of fluorescence change of NBD-taurine upon lowering the pH in RBC-GP4F complexes NBD-taurine-loaded RBC were bound to GP4F cells, washed, and suspended with trypsin-EDTA as described in Materials and Methods. 50 μl of the RBC-GP4F complex was injected into 2 ml PBS, pH 7.4, prewarmed at 37°C. About 1 min later, the pH in the medium was changed to 4.95 by adding 16 μl 0.5 M citrate (*bold arrow*). The anti-NBD quenches NBD fluorescence from the fluorophore leaked into the medium. Curves with and without antibody are marked as such. The curve indicating fluorescence from RBC-GP4F complexes lifted with chymotrypsin (HAo control) is marked HAo (pH-triggered; *bold arrow*).

et al., 1980; Blumenthal, 1987; Morris et al., 1988). Here we describe a new assay for cell–cell fusion in which both cytoplasmic-mixing and lipid-mixing are monitored continuously. Previously, aqueous and lipid fluorophores have been used separately to assay cell fusion (Keller et al., 1977; Wojcieszyn et al., 1983; Hoekstra and Klappe, 1986; Kempf et al., 1987; Ahkong et al., 1987; Sowers, 1987). However, in most of those studies fusion yields were calculated by counting all events in which fluorescence from a labeled membrane or the cytoplasm had moved to an unlabeled membrane or cytoplasm. The novelty with the approach presented in this paper is that the cells were continuously monitored before and during fusion. The monitoring was done on single cells by low light level video microscopy, as well as on a population of cells by spectrofluorometry. Moreover, we demonstrated the simultaneous redistribution of two fluorophores, reporting different criteria of fusion. This study revealed the following new observations and insights into HA-induced cell fusion: (*a*) continuous monitoring of fluorescence changes using two different criteria for fusion showed that when fusion is rapid, the maximal extent is reached within minutes; (*b*) the correspondence of the kinetics of the aqueous and lipid probes indicates that the cytoplasmic connections form as rapidly as the outer bilayers mix and there is no long-lived "partial-fusion" intermediate; (*c*) movement of fluorophores between effector and target was restricted during the initial events in fusion, consistent with the opening of small junctional pore(s); and (*d*) HA-induced leakage of a small molecule from the target occurred concomitant with fusion.

We were concerned about the R18 assay, since the dye might not be incorporated into the RBC bilayer membrane, but stably adsorbed to the RBC surface as micelles. However, the images in Fig. 3 *A* indicate diffusion of R18 over the RBC surface. This observation is consistent with fluorescence photobleaching recovery measurements of R18 directly incorporated into human RBC (Aoreti and Henis, 1987). A diffusion coefficient of (3.2 ± 0.5) × 10^{-9} cm^2/s at 22°C was measured with 0.94 mobile fraction, indicating incorporation of R18 into the RBC bilayer and free diffusion over its surface. This measured diffusion coefficient is within the range of that calculated from R18 movement seen in the images of Fig. 3 *A*.

Membrane Permeability Changes during Fusion

The two fusing membranes are in fact bounded by three aqueous compartments, two of whose contents mix as shown by the NBD-taurine assay. If there is also spill over to the third compartment, the fusion is "leaky." It is well known that fusion of influenza virus with the plasma membrane seems to be accompanied by immediate and profound changes in the passive permeability of the target membranes and red cell hemolysis (Pasternak et al., 1982; Loyter et al., 1988). Those permeability changes are induced by HA in intact virions and isolated HA aggregates (Sato et al., 1983), and by HA reconstituted in viral envelopes (Lapidot et al., 1987). Since we observed 30% NBD-taurine leakage during HA-induced fusion (Fig. 4), it appears that HA expressed on the surface of the 3T3 cells will also induce permeability changes in the RBC membrane. We do not know if the leakage occurs at the fusion site or some other permeability pathway in membranes. However, it shows the same specificity (HAo control), pH-dependence, and kinetics as fusion. Patel and Pastenak (1985) reported that influenza virus–induced leakage of cellular contents could be inhibited by adding 20 mM Ca^{2+} to the medium. The divalent cation at those con-

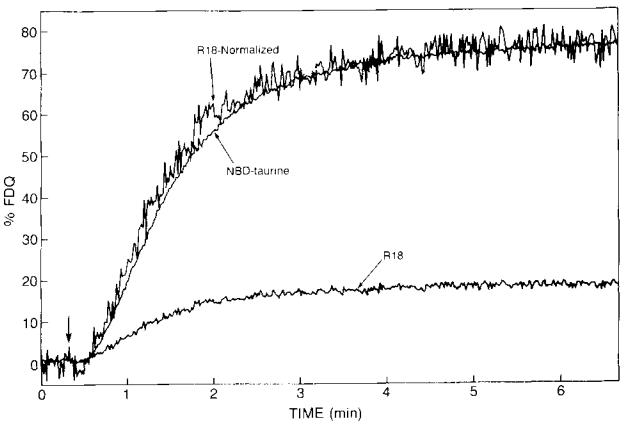

Figure 5. Comparison of cytoplasmic-mixing versus lipid mixing RBCs were double-labeled with NBD-taurine and R18. RBC-GP4F complexes were formed, washed, and suspended as described in the legend to Fig. 4. Fusion was triggered by lowering the pH to 5.0. (*bold arrow*). FDQ was calculated according to Eq. 1. The NBD-taurine curve (marked as such) was corrected for leakage according to Eq. 10 in Appendix I. The R18 curve was normalized to the maximal extent of NBD-taurine FDQ. Note similar lag time and sigmoidicity for the normalized R18 and NBD-taurine.

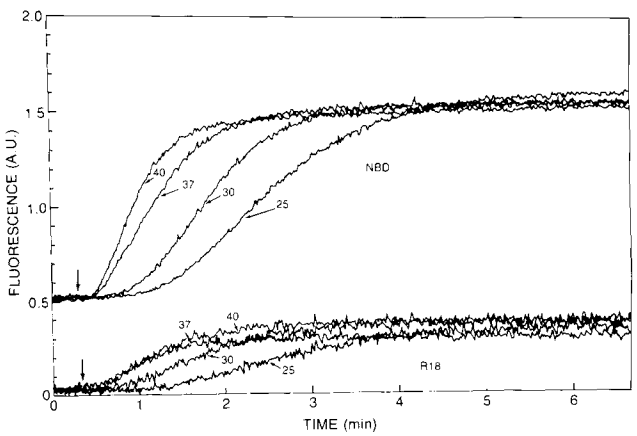

Figure 6. Temperature dependence of HA-induced cell fusion. RBCs were double-labeled with NBD-taurine and R18. RBC-GP4F complexes were formed, washed, and suspended as described in the legend to Fig. 4. 50 μl of the R18RBC-GP4F complex was injected into a cuvette containing 2 ml PBS, pH 7.4, prewarmed to different temperatures (*arrows*) using a circulating waterbath. About 1 min later, the pH in the medium was lowered to pH 5.0 (*bold arrows*). Upper curves and lower curves are NBD and R18 fluorescence changes, respectively.

centrations did not affect fusion or leakage in the GP4F–RBC system (data not shown).

No hemolysis of the RBC attached to the GP4F was seen during fusion (data not shown). Because of the colloid osmotic pressure of hemoglobin, we would expect a permeability change in the RBC membrane to result in swelling of the RBC. This was indeed observed. The fact that RBC swelling did not result in lysis indicates either that the permeability change was small and/or transient, or that a large area of continuity between the cytosols of RBC and GP4F was rapidly established. We observed the same kinetics of fluorescence dequenching when RBC–GP4F fusion was activated by lowering the pH in hyperosmotic solutions as under isoosmotic conditions (data not shown), indicating that the swelling is not a necessary condition for fusion. This is consistent with the observation that neither intact influenza virus–cell fusion, nor influenza virus–induced fusion of RBC ghosts depends on osmotic forces (Herrmann et al., 1988). Swelling is also seen in the case of membrane fusion during exocytosis. However, a careful examination of the sequence of events in exocytosis of secretory granules in mast cells demonstrate that swelling follows fusion and cannot be causal to fusion (Zimmerberg et al., 1987).

Diffusion of the Fluorophores in Single Cells

Using video microscopy, we observe movement of both dyes from single RBC to GP4F after lowering the pH (Fig. 3). The occurrence of a single fusion event should follow a pH-dependent probability distribution analogous to the voltage-dependent probability distribution of single channel openings in nerve membranes (Blumenthal, 1988). Theoretically, probability distributions can be determined from observation of many single fusion events. However, the time lag for the onset of dye movement for a single event cannot be predicted from the time lag for the onset of FDQ in a population of cells.

The pattern of dye redistribution into GP4F cells after onset of movement of R18 and NBD-taurine was different. After crossing the RBC-GP4F barrier, NBD-taurine immediately redistributed homogeneously throughout the GP4F cell, whereas, with R18, homogeneous redistribution over the GP4F cell membrane was only seen after ~60 s. Redistribution times (τ) can be estimated from the diffusion coefficient (D) and the radius (r), according to Eqs. 2 a and 2 b for the two-dimensional diffusion over the surface of the cell and the three-dimensional diffusion through the cytoplasm, respectively:

$$\tau = (r)^2/4D \qquad (2\text{ a})$$

$$\tau = (r)^2/6D. \qquad (2\text{ b})$$

The radius of the GP4F cell is $\sim 10^{-3}$ cm. By fluorescence photobleaching recovery, a diffusion coefficient of 0.32×10^{-8} cm^2/s has been measured for R18 in human RBC at 22°C (Aoreti and Henis, 1986). Inserting 2.4 times that value to estimate D at 37°C, we calculate from Eq. 2 a a redistribution time of 33 s for R18. On the other hand, estimating $D = 5 \times 10^{-6}$ cm^2/s for NBD-taurine (diffusion coefficient of a molecule with the same molecular weight (sucrose, 340), the τ for redistribution is calculated from Eq. 2 b to be ~0.03 s for NBD-taurine. The redistribution time for R18 after cell fusion yields the same value for the diffusion coefficient of a lipid as that reported using a variety of biophysical techniques (Edidin, 1987). Interestingly, the first measurement of diffusion of molecules on cell surfaces was made using viral-induced cell fusion techniques (Frye and Edidin, 1970).

Although homogeneous redistribution of NBD-taurine throughout the GP4F cell occurred immediately after crossing the barrier, the total NBD fluorescence in the GP4F cells increased relatively slowly (Fig. 3 *B*). This is because of limited permeability of the molecule across the junction formed by fusion complexes (see below).

The observation by video microscopy that redistribution of both aqueous and lipid fluorophores on single cells is slow may lead to the conclusion that the lag time observed by spectrofluorometry results from the fact that probe diffusion is the rate-limiting step in the observed fluorescence changes associated with RBC–GP4F fusion. However, the correspondence between lag times using two entirely different assays argues against such an interpretation. Moreover, the temperature dependence of probe diffusion is not likely to give rise to the fivefold difference in lag time between 25°C and 37°C (Fig. 6).

Mechanisms of HA-induced Membrane Fusion

We have previously analyzed mechanisms of membrane fusion mediated by viral spike glycoproteins in the framework of effects of pH-induced conformational changes and cooperativity on the protein's ability to induce fusion (Blumenthal, 1988; Blumenthal et al., 1988). A formalism has been derived based on a model in which the viral spike glycoproteins are assumed to be arranged as oligomers; i.e., they consist of a number of subunits that can undergo a "concerted" conformational change from an inactive state to an active state. Each subunit in the oligomer contains a regulatory site for

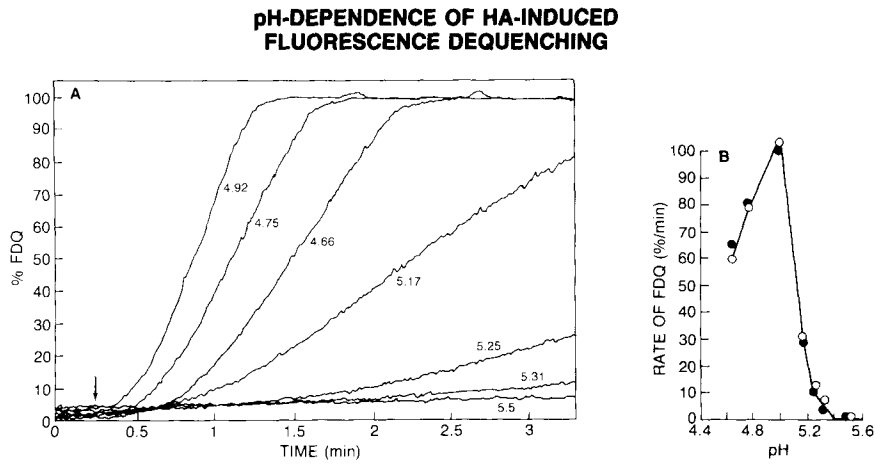

Figure 7. pH-dependence of fluorescence dequenching of NBD-taurine in RBC-GP4F complexes. (*A*) NBD-taurine-loaded RBC were bound to GP4F cells, washed, and suspended with trypsin-EDTA as described in the legend to Fig. 4. 50 μl of the RBC-GP4F complex was injected into 2 ml PBS, pH 7.4, and prewarmed at 37°C. About 1 min later, the pH in the medium was changed as indicated by adding 16 μl 0.5 M citrate (*arrow*). (*B*) The maximal rate of FDQ; (●) NBD-taurine; (○) R18.

a ligand; binding the ligand induces a conformational change towards the active form thereby enabling the fusion process to occur. In the case of HA, the model assumes that protonation of three subunits of the trimer leads to a concerted conformational change to the activated form (Boulay et al., 1988). A number of those activated trimers then come together to form a fusion junction (Blumenthal et al., 1988). This can be regarded as a "gating" process that allows flow of lipid between membranes and of aqueous contents between previously enclosed spaces. The putative junction formation would be equivalent to the exocytotic pore formation observed during fusion of secretory granules (Chandler and Heuser, 1980; Ornberg and Reese, 1981; Zimmerberg et al., 1987; Breckenridge and Almers, 1987).

Our observations of aqueous content mixing using low light level video microscopy on single cells enable us to examine the nature of the fusion junction. In Appendix II, we have derived an expression for the rate constant k for movement of an aqueous marker through one or more fusion junctions of a given pore radius (ρ). Although homogeneous redistribution of NBD-taurine throughout the GP4F cell occurred immediately after crossing the barrier, the total NBD fluorescence in the GP4F cells increased with a half-time of ~25 s, or k = 0.028/s (see Fig. 3 *B*). For a small marker such as NBD-taurine with a diffusion coefficient of 5×10^{-6} cm²/s, that rate constant is consistent with formation of 1 junction with ρ = 4.5 nm, 5 junctions with ρ = 2.0 nm, or 20 junctions with ρ = 1.0 nm (see Appendix II; Eq. 4).

In its overall shape, hemoglobin resembles a spheroid with length 6.4, width 5.5 nm, and height 5.0 nm (Perutz, 1969). Therefore, a ρ of 4.5 nm would not be sufficiently large for free permeation of that macromolecule. Little or no hemoglobin movement from the RBC to the GP4F cell was seen within 10 min. Doxsey et al. (1985) reported a similar observation for large molecules such as horse radish peroxidase or immunoglobulin that were encapsulated in resealed RBC ghosts fusing to HA-expressing 3T3 cells. If the initial opening were 100 nm (the smallest cytoplasmic continuity junction seen by EM, Doxsey et al., 1985), then NBD-taurine redistribution would occur with 0.1 s. Therefore, we conclude that movement of fluorophores between effector and target is restricted during the initial events in fusion, consistent with the opening of small junctional pore(s). At later stages of the fusion process, we expect these pores to widen, as we observed in mast cell exocytosis (Zimmerberg et al., 1987). The initial number and size of junctions formed during HA-mediated fusion, as well as the development of the pore(s), will be examined in more detail using markers of different size incorporated into the RBC, and by whole cell capacitance patch clamp techniques.

Appendix I

Derivation of Correction for NBD-taurine Leakage upon Fusion

Definitions:

a = moles of NDB-taurine in RBC;
b = moles in RBC-GP4F (fused complexes);
c = moles leaked out (upon fusion);
$n = a + b + c$ (total moles of NBD-taurine).

fl = "intrinsic" fluorescence of NBD-taurine in RBC;
$f2$ = "intrinsic" fluorescence in fused complex = fluorescence in medium.

F = measured fluorescence at time t;
F_0 = measured fluorescence at time 0;
F_t = measured fluorescence after detergent addition (completely dequenched);
F_a = measured fluorescence at time t in the presence of antibody.

Assumptions:

(*1*) in the presence of antibody fluorescence in the medium ($f2$) = 0;
(*2*) no initial leakage (at time = 0);
(*3*) instantaneous fluorescence change fl → f2 upon fusion/leakage;
(*4*) backgrounds are the same in the presence of Antibody or detergent.

Equations:

$F = afl + bf2 + cf2$ (1)
$F_0 = nfl = (a + b + c)fl$ (2)
$F_t = nf2 = (a + b + c)f2$ (3)
$F_a = afl + bf2$. (4)

Combine Eqs. 1 and 2:

$F - F_0 = (b + c)(f2 - fl)$. (5)

Combine Eqs. 1 and 3:

$F_t - F_0 = n(f2 - fl)$. (6)

Combine Eqs. 5 and 6:

$(b + c)/n = (F - F_0)/(F_t - F_0)$ (7) (fraction fused + leaked).

Combine Eqs. 1 and 4:

$F - Fa = cf2$. (8)

Combine Eqs. 8 and 2:

$c/n = (F - Fa)/F_t$ (9) (fraction leaked).

To get the fraction of molecules in fused structures, subtract Eq. 9 from Eq. 7:

$b/n = ((F - F_0)/(F_t - F_0)) - ((F - Fa)/Ft)$. (10)

Appendix II

Calculation of the size and/or number of "fusion pores"

If an RBC becomes completely permeabilized, the permeability coefficient (P) for a given molecule will be given by:

$$P = D/\delta, \quad (1)$$

where D is its diffusion coefficient, and δ the length of the pathway for diffusion.

If instead of complete permeabilization the appositional area of the RBC membrane is perforated with n pores with radius ρ, then the permeability will be given by Eq. 1 multiplied by the fractional area the RBC membrane occupied by pores:

$$P = (D/\delta) \times (n\pi\rho^2)/(\pi r^2), \quad (2)$$

where r is the radius of the RBC. The rate constant (k) for movement of molecules from the RBC can be calculated from the permeability according to:

$$k = AP/V, \quad (3)$$

where V and A are volume and appositional area of the RBC, respectively. For an attached hemispherical cell (see Figs. 1 and 3), $V/A = 2r/3$. Inserting that value, and combining Eq. 2 and 3 yields:

$$n\rho^2 = (0.67 \times r^3 \times \delta \times k)/D, \quad (4)$$

If we take the RBC radius to be 3.4 μm, D to be 5×10^{-6}cm^2/s, δ to be 1.4×10^{-6}cm (length of HA), and k to be 0.028/s, then formation of 1 junction would yield $\rho = 4.5$ nm; 5 junctions, $\rho = 2.0$ nm; or 20 junctions, $\rho = 1.0$ nm.

Anti-NBD antibody was kindly provided by Dr. Z. I. Cabantchik. We thank Drs. A. Puri, J. Lowy, and R. W. Doms for many helpful suggestions. We are very grateful to Dr. J. M. White for generously providing the GP4F cells and for her many helpful suggestions.

Received for publication 20 December 1988 and in revised form 30 March 1989.

References

Ahkong, Q. F., J. P. Desmazes, D. Georgescauld, and J. A. Lucy. 1987. Movements of fluorescent probes in the mechanism of cell fusion induced by poly(ethylene glycol). *J. Cell Sci.* 88:389–398.

Aroeti, B., and Y. I. Henis. 1987. Fusion of native Sendai virions with human erythrocytes. Quantitation by fluorescence photobleaching recovery. *Exp. Cell Res.* 170:322–337.

Blumenthal, R. 1987. Membrane Fusion. *Curr. Top. Membr. Transp.* 29:203–254.

Blumenthal, R. 1988. Cooperativity in Viral Fusion. *Cell Biophys.* 12:1–12.

Blumenthal, R., A. Puri, D. P. Sarkar, Y. Chen, O. Eidelman, and S. J. Morris. 1988. Membrane fusion mediated by viral spike glycoproteins. *UCLA (Univ. Calif. Los. Angel.) Symp. Mol. Cell. Biol. New Ser.* 90:197–217.

Blumenthal, R., A. Bali-Puri, A. Walter, D. Covell, O. Eidelman. 1987. pH-Dependent fusion of vesicular stomatitis virus with vero cells: measurement by dequenching of octadecylrhodamine fluorescence. *J. Biol. Chem.* 262: 13614–13619.

Boulay, F., R. W. Doms, R. Webster, and A. Helenius. 1988. Posttranslational oligomerization and cooperative acid activation of mixed influenza hemagglutinin trimers. *J. Cell Biol.* 106:629–639.

Breckenridge, L. J., and W. Almers. 1987. Currents through the fusion pore that forms during exocytosis of a secretory vesicle. *Nature (Lond.).* 328:814–817.

Cabantchik, Z. I., and A. Rothstein. 1972. The nature of the membrane sites controlling anion permeability of human red blood cells as determined by studies with disulfonic stilbene derivatives. *J. Membr. Biol.* 10:311–330.

Chandler, D. E., and J. E. Heuser. 1980. Arrest of membrane fusion events in mast cells by quick-freezing. *J. Cell Biol.* 86:666–674.

Choppin, P. W., and A. Scheid. 1980. The role of viral glycoproteins in adsorption, penetration, and pathogenicity of viruses. *Rev. Infect. Dis.* 2:40–58.

Darmon, A., O. Eidelman, and Z. I. Cabantchik. 1982. A method for measuring anion transfer across membranes of hemoglobin-free cells and vesicles by continuous monitoring of fluorescence. *Anal. Biochem.* 119:313–321.

Doxsey, S. J., J. Sambrook, A. Helenius, and J. White. 1985. An efficient method for introducing macromolecules into living cells. *J. Cell Biol.* 101:19–27.

Edidin, M. 1987. Rotational and lateral diffusion of membrane proteins and lipids: phenomena and function. *Curr. Top. Membr. Transp.* 29:91–127.

Eidelman, O., and Z. I. Cabantchik. 1980. A method for measuring anion transfer across red cell membranes by continuous monitoring of fluorescence. *Anal. Biochem.* 106:335–341.

Eidelman, O., M. Zangvill, M. Razin, H. Ginsburg, and Z. I. Cabantchik. 1981. The anion-transfer system of erythrocyte membranes. N-(7-Nitrobenzofurazan-4-yl)taurine, a fluorescent substrate-analogue of the system. *Biochem. J.* 195:503–513.

Frye, L. D., and M. Edidin. 1970. The rapid intermixing of cell surface antigens after formation of mouse-human heterokaryons. *J. Cell Sci.* 7:319–335.

Giloh, H., and J. W. Sedat. 1982. Fluorescence microscopy: reduced photobleaching of rhodamine and fluorescein protein conjugates by n-propyl gallate. *Science (Wash. DC).* 217:1252–1255.

Herrmann, A., C. Pritzen, A. Palesch, and T. Groth. 1988. The influenza virus-induced fusion of erythrocyte ghosts does not depend on osmotic forces. *Biochim. Biophys. Acta.* 943:411–418.

Hoekstra, D., and K. Klappe. 1986. Use of a fluorescence assay to monitor the kinetics of fusion between erythrocyte ghosts, as induced by Sendai virus. *Biosc. Rep.* 6:953–960.

Hoekstra, D., T. de Boer, K. Klappe, and J. Wilschut. 1984. Fluorescence method for measuring the kinetics of fusion between biological membranes. *Biochemistry.* 23:5675–5681.

Keller, P. M., S. Person, and W. Snipes. 1977. A fluorescence enhancement assay of cell fusion. *J. Cell Sci.* 28:167–177.

Kempf, C., M. R. Michel, U. Kohler, and H. Koblet. 1987. A novel method for the detection of early events in cell-cell fusion of Semliki Forest virus infected cells growing in monolayer cultures. *Arch. Virol.* 95:283–289.

Klenk, H. D., R. Rott, M. Orlich, and J. Blodorn. 1975. Activation of influenza A viruses by trypsin treatment. *Virology.* 68:426–439.

Lapidot, M., O. Nussbaum, and A. Loyter. 1987. Fusion of membrane vesicles bearing only the influenza hemagglutinin with erythrocytes, living cultured cells, and liposomes. *J. Biol. Chem.* 262:13736–13741.

Loyter, A., O. Nussbaum, and V. Citovsky. 1988. Active function of membrane receptors in fusion of enveloped viruses with cell plasma membranes. *In* Molecular Mechanisms of Membrane Fusion. S. Ohki, D. Doyle, T. Flanagan, S. W. Hui, and E. Mayhew, editors. Plenum Publishing Corp., New York. 413–426.

Morris, S. J., D. Bradley, G. C. Gibson, P. D. Smith, and R. Blumenthal. 1988. Use of membrane-associated fluorescence probes to monitor fusion of vesicles. *In* Spectroscopic Membrane Probes, Volume I. L. Loew, editor. CRC Press Inc., Boca Raton, FL. 161–191.

Morris, S. J., D. P. Sarkar, J. M. White, and R. Blumenthal. 1989. Kinetics of pH-dependent fusion between 3T3 fibroblasts expressing influenza hemagglutinin and red blood cells: measurement by dequenching of fluorescence. *J. Biol. Chem.* 264:3972–3978.

Ornberg, R. L., and T. S. Reese. 1981. Beginning of exocytosis captured by rapid-freezing of limulus amebocytes. *J. Cell Biol.* 90:40–54.

Pasternak, C. A., M. A. Gray, and K. J. Micklem. 1982. Membrane changes during viral infection. *Biosci. Rep.* 2:609–612.

Patel, K., and C. A. Pasternak. 1985. Permeability changes elicited by influenza and Sendai viruses: separation of fusion and leakage by pH-jump experiments. *J. Gen. Virol.* 66:767–775.

Perutz, M. F. 1969. Structure and function of hemoglobin. *Harvey Lect.* 63:213–261.

Sambrook, J., L. Rodgers, J. White, M.-J. Gething. 1985. Lines of BPV-transformed murine cells that constitutively express influenza virus hemagglutinin. *EMBO (Eur. Mol. Biol. Organ.) J.* 4:91–103.

Sato, S. B., K. Kawasaki, and S. Ohnishi. 1983. Hemolytic activity of influenza virus hemagglutinin glycoproteins activated in mildly acidic environments. *Proc. Natl. Acad. Sci.* 80:3153–3157.

Sowers, A. E. 1987. The long-lived fusogenic state induced in erythrocyte ghosts by electric pulses is not laterally mobile. *Biophys. J.* 52:1015–1020.

Wiley, D. C., and J. J. Skehel. 1987. The structure and function of the hemagglutinin membrane glycoprotein of influenza virus. *Annu. Rev. Biochem.* 56:365–394.

White, J., K. Matlin, and A. Helenius. 1981. Cell fusion by Semliki Forest, influenza, and vesicular stomatitis viruses. *J. Cell Biol.* 89:674–679.

White, J., A. Helenius, and M.-J. Gething. 1982. Haemagglutinin of influenza virus expressed from a cloned gene promotes membrane fusion. *Nature (Lond.).* 300:658–659.

White, J., M. Kielian, and A. Helenius. 1983. Membrane fusion proteins of enveloped animal viruses. *Q. Rev. Biophys.* 16:151–195.

Wojcieszyn, J. W., R. A. Schlegel, K. Lumley-Sapanski, and K. A. Jacobson. 1983. Studies on the mechanism of polyethylene glycol-mediated cell fusion using fluorescent membrane and cytoplasmic probes. *J. Cell Biol.* 96:151–159.

Zimmerberg, J., F. C. Cohen, and A. Finkelstein. 1980. Fusion of phospholipid vesicles with planar bilayer membranes. I. Discharge of vesicular contents across the planar membrane. *J. Gen. Physiol.* 75:241–250.

Zimmerberg, J., M. Curran, F. S. Cohen, and M. Brodwick. 1987. Simultaneous electrical and optical measurements show that membrane fusion precedes secretory granule swelling during exocytosis of beige mouse mast cells. *Proc. Natl. Acad. Sci. USA.* 84:1585–1589.